Доклади на Българската академия на науките
Comptes rendus de l'Académie bulgare des Sciences

Tome 79, No 11, 2026

MATHEMATICS

Mechanics

FLOW-INDUCED INSTABILITY AROUND A SUBMERGED ELASTICALLY MOUNTED BLUFF BODY NEAR A FREE SURFACE

Grigor Nikolov✉, Dimitar Trukhchev, Rumen Kishev, Anton Anastasov

Received on February 11, 2026
Presented by S. Margenov, Corresponding Member of BAS, on September 29, 2026

Abstract

The stability of fluid flow and vortex formation processes around a bluff body (circular cylinder) submerged close beneath the free surface, has been investigated. The analysis was performed at subcritical and critical regimes according to Reynolds Re and Froude Fr numbers, characteristic for practical applications. The study covers ranges of $Re = 5 \times 10^3 - 25 \times 10^3$, (corresponding to subcritical flow conditions with a well-developed vortex street), and $Fr = 0.2 - 1.2$ (including both subcritical ($Fr < 1$) and critical ($Fr \approx 1$) modes of interaction with the free surface). The frequency characteristics of vortex formation are analyzed using the Struhal number in the range $St = 0.18 - 0.22$, with particular attention paid to the synchronization between the vortex shedding frequency and the natural frequency of the elastically mounted body. The dynamics of vortex-induced vibrations are described by the reduced velocity U^*, with the lock-in mode identified in the range $U^* = 4 - 8$. It has been found that a decrease in the relative immersion depth h/D together with the critical Froude numbers leads to a significant narrowing of the synchronization range, which noticeably reduces the amplitude of the induced vortex oscillations and lowers the energy potential. When the h/D values are decreasing, a mode is reached, in which the oscillations are completely suppressed and the

This research was carried out under the BAS Postdoctoral Procedure within task BG-RRP-2.015-0012-C01 Application of Computational Fluid Dynamics Methods in the Design of Energy-Saving Devices and the Deployment of Green Technologies in the Marine Industry.

https://doi.org/10.7546/CRABS.2026.11.03

flow is controlled mainly by the hydraulic jump and the strongly asymmetric distribution of the impulse.

Key words: flow instability, Reynolds number, vortex-induced vibrations, free surface, bluff body

2020 Mathematics Subject Classification: 76E30

Introduction. The flow around bluff submerged bodies, the occurrence of fluid instability, and the appearance of vortex-induced vibrations are classic problems in fluid mechanics that have important engineering applications. The physical mechanisms governing vortex formation and synchronization between the vortex shedding frequency and the natural frequency of the elastically mounted body are discussed in detail by [1, 2]. In a synchronization (lock-in) regime large-amplitude vibrations can be observed, which are essential for structural integrity [3] and can find specific practical applications, for example, for energy harvesting. The presence of a free surface in the vicinity of a bluff body introduces additional complexity by modifying both the near-wake structure and the global vortex dynamics. Early experimental studies demonstrated that a reduction in the relative submergence depth h/D leads to pronounced asymmetry in the vortex street and to significant changes in the vortex shedding frequency [4, 5]. More recent numerical investigations based on the Finite-volume method (FVM) combined with Volume-of-fluid free-surface (VOF) modelling (FVM+VOF) have shown that free-surface effects can significantly alter the extent of the lock-in region and the amplitude of vortex-induced vibrations [6, 7].

In parallel, mesh-free approaches, particularly smoothed particle dynamics (SPH), have emerged as powerful tools for the analysis of strongly nonlinear free-surface flows and fluid–structure interaction problems. Owing to their fully Lagrangian formulation, SPH methods are especially well suited for cases involving large free-surface deformations and hydraulic jumps [8, 9]. Recent studies indicate that, at elevated Froude numbers, the interaction between vortex shedding and the free surface may result in a suppression or abrupt termination of the lock-in regime, characterized by a rapid drop in oscillation amplitude rather than a gradual decay [10].

Experimental investigations remain an essential source for validating numerical predictions and for elucidating the physical mechanisms underlying the observed flow regimes. A combined framework incorporating FVM +VOF simulations, SPH modelling, and experimental measurements therefore provides a robust basis for characterizing flow instabilities and the vortex-induced response of a bluff body submerged near a free surface.

Despite recent advances, the influence of free-surface effects on the vortex-induced response of elastically mounted bluff bodies is not yet fully understood, particularly in sub-critical and critical Reynolds and Froude number regimes. The present study addresses this gap by providing a systematic characterization of flow

instabilities through a combined numerical and experimental approach.

Problem formulation and governing equations. Consider a circular cylinder of diameter D and span L submerged in an incompressible fluid of density ρ and kinematic viscosity ν. The cylinder is positioned at a vertical distance h below a deformable free surface and is subjected to a uniform incoming flow with velocity U_∞. The cylinder is elastically mounted and allowed to oscillate in both the inline and transverse directions. A schematic illustration of the physical configuration and the elastic support system is presented in Fig. 1a. The computational domain together with the corresponding mesh is shown in Fig. 1b. The upper, lower, left, and right boundaries are treated as symmetry planes, while prescribed velocity and pressure conditions are imposed at the inlet and outlet, respectively. The cylinder surface is modelled as a no-slip wall. Fluid-structure interaction is represented using a dynamic mesh approach, allowing the computational domain to deform consistently with the cylinder motion.

The fluid motion is governed by the three-dimensional incompressible Navier–Stokes equations. The velocity field is described by the vector $\mathbf{u} = (u, v, w)$, while p denotes the pressure. Assuming incompressible flow, the governing equations are

$$\nabla \cdot \mathbf{u} = 0, \tag{1}$$

$$\frac{\partial \mathbf{u}}{\partial t} + \mathbf{u} \cdot \nabla \mathbf{u} = -\frac{1}{\rho} \nabla p + \nu \nabla^2 \mathbf{u} + \mathbf{g}, \tag{2}$$

where $\mathbf{g} = (0, 0, -g)$ is the gravitational acceleration. For free-surface flows, the interface between water and air is represented by the phase-fraction field $\alpha(\mathbf{x}, t)$ satisfying

$$\frac{\partial \alpha}{\partial t} + \mathbf{u} \cdot \nabla \alpha = 0. \tag{3}$$

The governing non-dimensional parameters describing the fluid-structure interaction problem are

$$\left(Re,\, Fr,\, U^*,\, St,\, Co,\, \frac{A}{D},\, \tau \right) = \left(\frac{UD}{\nu},\, \frac{U}{\sqrt{gD}},\, \frac{U}{f_n D},\, \frac{f_s D}{U},\, \frac{U \Delta t}{\Delta x},\, \frac{A}{D},\, \frac{t U_\infty}{D} \right).$$

Here, Re is the Reynolds number, Fr is the Froude number, U^* is the reduced velocity, St is the Strouhal number, Co is the Courant number, A/D denotes the normalized vibration amplitude, and τ is the dimensionless time. The vortex shedding process is characterized by the shedding frequency f_s, while the lock-in phenomenon occurs when the shedding frequency approaches the natural frequency of the oscillating system.

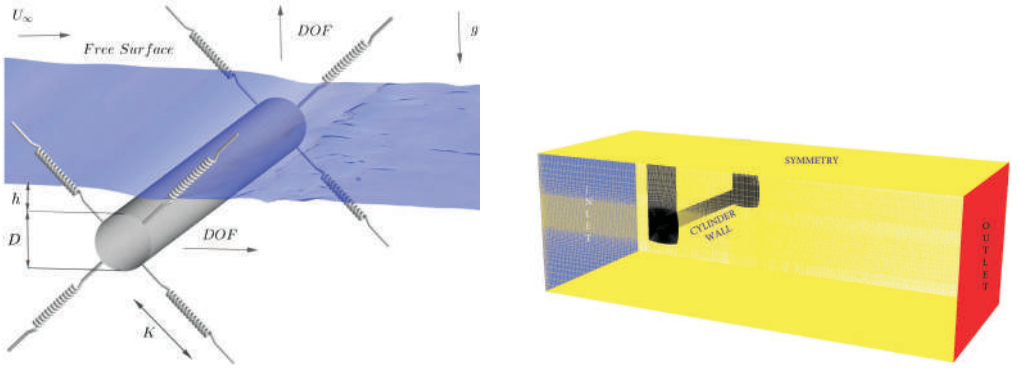

a) b)

Fig. 1. Scheme of the study: a) elastically mounted circular cylinder near a free surface; b) computational domain and definition of the inline and transverse degrees of freedom (DOF)

The vibration response of the cylinder is described by a two-degree-of-freedom mass-spring-damper oscillator

$$m_{\text{eff}}\ddot{q}_i(t) + c_i\dot{q}_i(t) + k_i q_i(t) = F_i(t), \qquad q_i \in \{x, y\},$$

$$m_{\text{eff}} = m + m_a(h/D), \qquad f_{n,i} = \frac{1}{2\pi}\sqrt{\frac{k_i}{m_{\text{eff}}}}.$$

Here, m_{eff} is the effective oscillating mass, consisting of the structural mass m and the hydrodynamic added mass m_a, which depends on the normalized submergence depth h/D. The variables $x(t)$ and $y(t)$ denote the inline and transverse displacements, respectively, c_i and k_i are the damping and stiffness coefficients, and $F_i(t)$ represents the corresponding hydrodynamic excitation force. The natural frequency $f_{n,i}$ governs the structural response of the oscillator, whereas the vortex shedding frequency f_s characterizes the wake dynamics and determines the occurrence of synchronization (lock-in).

Features of the numerical implementation. The numerical investigation combines the Finite Volume Method (FVM) and Smoothed Particle Hydrodynamics (SPH) to simulate the fluid–structure interaction between the oscillating cylinder and the deformable free surface. The finite-volume simulations employ an Eulerian formulation with the Volume-of-Fluid (VOF) method for free-surface capturing, whereas the SPH approach provides a fully Lagrangian description of the flow. The computational mesh was generated following the ITTC Recommended Procedures and Guidelines [11], with local refinement around the cylinder, free surface, and wake region.

Turbulence was modelled using a Wall-Modelled Large Eddy Simulation (WMLES) approach [13]. The convective and diffusive terms were discretized

using second-order schemes, while time integration employed a second-order implicit method. The time step was selected to satisfy $Co < 1$, and convergence at each time step was achieved when the residuals fell below 2×10^{-4}.

The finite-volume simulations were performed using OpenFOAM and ANSYS Fluent, whereas the SPH simulations were carried out using DualSPHysics. The combined Eulerian and Lagrangian approaches provide complementary predictions of the flow field, free-surface evolution, and vortex-induced vibration response. The numerical models were validated against the experimental measurements obtained under identical flow conditions. The comparison included the cylinder vibration amplitudes, oscillation frequencies, and vortex shedding characteristics. The computational mesh was generated following the ITTC Recommended Procedures and Guidelines [11]. Grid independence was verified using three systematically refined meshes, while temporal convergence was confirmed through a time-step sensitivity study. The selected mesh and time step provided mesh-independent and temporally converged solutions.

In the course of the numerical experiments, a qualitative agreement and quantitative closeness were achieved between the numerical results and those from the experimental observations, which serves as an additional criterion for the adequacy of the numerical algorithm used to reproduce the interactions between the fluid and the structure, as well as the dynamics of the free surface.

Laboratory methods used in the experimental study of a scaled physical model. Another series of experimental studies was conducted in the cavitation tunnel at the Institute of Metal Science, Equipment and Technologies with Hydro- and Aerodynamics Centre "Acad. A. Balevski" at the Bulgarian Academy of Sciences. The technical facility includes the cavitation tunnel, the test section with a flexibly mounted circular cylinder, and the QUALISYS optical motion capture system. The tests were conducted under uniform inflow conditions at various Reynolds numbers and relative submergence ratios (h/D). The cylinder mounting system allows oscillations in the inline and transverse directions. Its dynamic response was measured using the QUALISYS optical motion-capture system, while flow visualization was performed using stroboscopic illumination and fine air bubbles to observe the vortex shedding process, wake development, and free-surface deformation. The results of this type of research (so-called experimental fluid dynamics EFD) on the response to vortex-induced vibrations are independent in nature, but at the same time provide a natural basis for model parameters tuning and validating the results in numerical experiments described above.

Results and discussion. A visualization of a part of the temporal evolution of the vortex street (over two oscillation periods) generated in the wake of the cylinder at $Re = 19350$ and initial $h/D = 0.5$ is shown in Fig. 2. In the model-scale experiments, the vortices are tracked visually using air bubbles introduced into the water immediately downstream of the cylinder. These bubbles are entrained

by the generated vortices in the direction of the flow and, at later times, rise toward the free surface and are released into the atmosphere.

In the numerical simulations the vortical structures are identified at the boundary of the computational domain. In Fig. 2b they are represented according to the $Q_{criteria}$ with iso-surfaces, defined as contours of a second eigenvalue of the tensor $s^2 + \omega^2$, where s and ω are the strain and the rotation of velocity field, respectively, and $Q_{criteria} = -0.001$ [14]. Figure 2a, b provides a qualitative comparison between EFD and CFD results. The red circles denote regions of intensified vortical activity and wake asymmetry, which are captured consistently by both experimental observations and numerical simulations.A good quantitative agreement between EFD and CFD is also achieved with respect to the dominant shedding frequency and phase.

In Fig. 2c the flow structures are visualized using the rotation $\omega = \partial U_x/\partial y - \partial U_y/\partial x$, which represents the out-of-plane vorticity component. For unsteady flow conditions, the visualization of particle trajectories (streak-lines) at a given time t is obtained by releasing a set of particles with initial position x_0 at times $s \in [t_{\min}, t]$, after which the particle positions are computed up to time t according to $x_{\text{streak}}(s; x_0, t) = x_{\text{path}}(t; x_0, s)$. The streak-line is parameterized by s, while $t_{\min}$ denotes the initial particle release time. This approach is employed in the SPH simulations to visualize the temporal evolution of the flow in Fig. 2c.

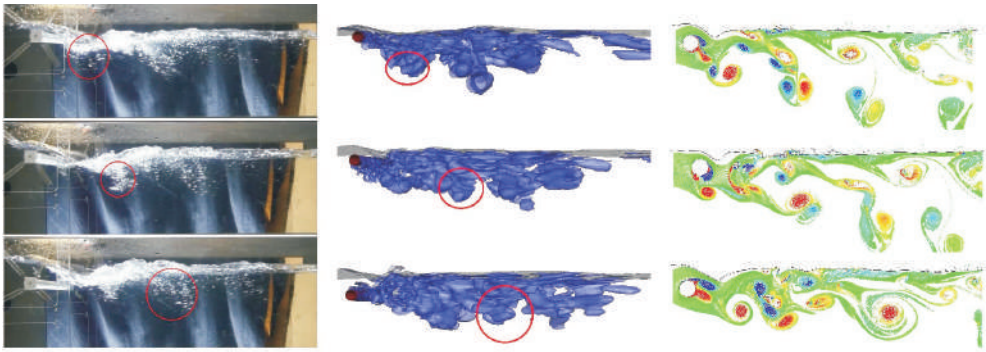

Fig. 2. Evolution of the vortex street at $Re = 19350$ and initial $h/D = 0.5$ based on results from: a) EFD; b) FVM + SPH; c) SPH

The asymmetric nature of vortex shedding implies differences in the forces generated along the cylinder and, consequently, differences in the normalized vibration amplitudes A/D between the fully submerged case ($h/D = 3$) and a cylinder located near the free surface ($h/D = 0.5$). This behaviour is consistently observed in both the model-scale experiments and the numerical simulations, as illustrated in Fig. 2.

It should also be noted that the transition of the system to blocking mode requires additional time, which significantly increases the total duration of the

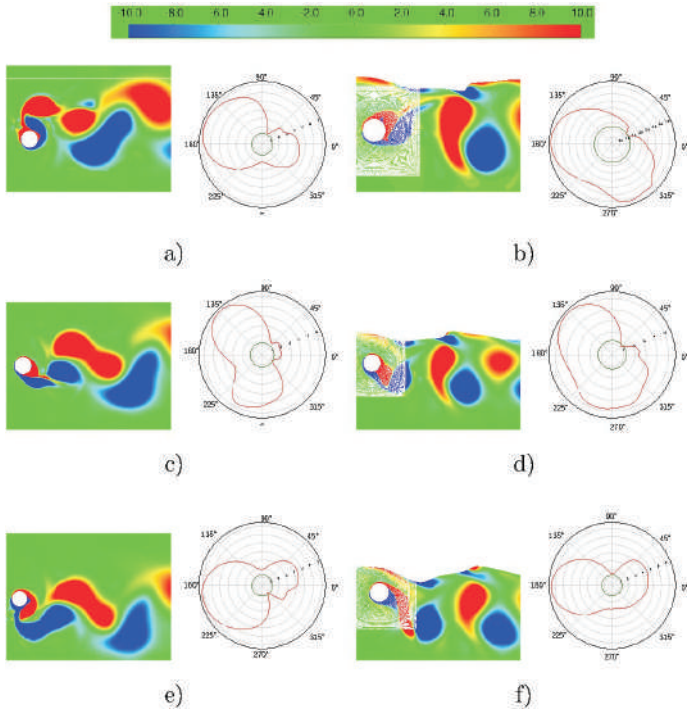

Fig. 3. Influence of absence (a, c, e) or taking into account of the free surface (b, d, f) on pressure field and vortex shedding processes for initial $h/D = 1$. Three sequence changes in cylinder oscillations are shown

simulations. Figure 4 clearly shows that, in some cases ($Re_D = 21125$, $h/D = 1$), the onset of synchronization may take more than 6 s astronomical time. The graphs in Fig. 4a demonstrate the complete suppression of vortex-induced vibrations at $Re = 21125, h/D = 0.45$ and $U^* = 9.71$, in comparison with a stable oscillatory regime maintained at $Re = 18750$, $h/D = 1$ and $U^* = 8.75$. The amplitude of transverse oscillations decreases when the steady state of the process is reached, but the reason for this is different: at low Froude numbers, it is the Coanda effect, while at Fr close to critical values, it is the influence of the highly corrugated free surface. An instantaneous state of the flow field at $\tau = 8$ for $Re = 21125$ and $Fr_h = 3.61$ is shown in Fig. 4b. It is evident that vortex shedding is suppressed due to the combined influence of several factors leading to the onset of a bifurcation. It can also be noted that surface waves generated as a consequence of absolute instability induced by the proximity of the cylinder to the free surface are present and may be considered among the contributing factors influencing the bifurcation process.

The distribution of the pressure coefficient $C_p = (p - p_\infty)/(0.5\,\rho U_\infty^2)$ as a function of vortex shedding and submergence depth, shown in polar (azimuthal)

coordinates over one oscillation cycle, for the case without a free surface and for initial $h/D = 1$, is presented in Fig. 3. The results indicate that the presence of a free surface modifies the vortex formation process and the associated pressure distribution on the polar surface by shifting the azimuthal location of the critical vortex-shedding point, thereby affecting the oscillatory response of the submerged cylinder.

The differences in the physics of the processes in the different variants depending on the submersion depth of the cylinder and the flow velocity are clearly shown in Fig. 4c. The range of reduced speeds at which synchronization with locking is achieved decreases as the cylinder approaches the free surface, thereby reducing the amplitude of vibrations A/D due to the partial or complete shedding of vortex separation.

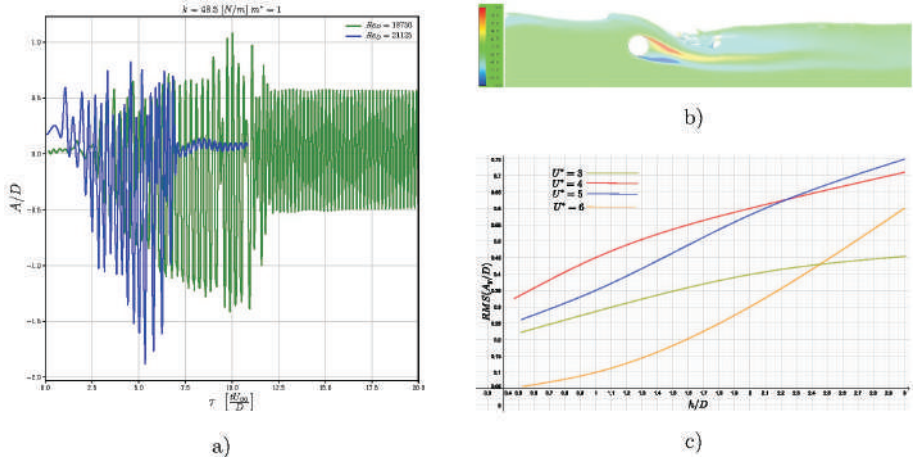

Fig. 4. Influence of input parameters on the oscillation regime: a) Abrupt loss of stability of transverse oscillations when varying in time τ from $h/D = 1$, $U = 0.75$ m/s, $U^* = 8.75$, and $Re = 18750$ (green) to $h/D = 0.45$, $U = 0.85$ m/s, $U^* = 9.71$, and $Re = 21125$ (blue); b) A regime of complete suppression of vortex shedding at $Fr_h = 3.61$, $Re = 21125$, $U^* = 9.71$; c) Root-mean-square vertical displacement of the oscillating cylinder for different values of U^* and h/D between 3 – 6 and 0.4 – 3, respectively

Conclusion. The main generalized conclusions can be summarized as follows. A decrease in the submergence ratio h/D results in a reduction of the normalized vibration amplitude A/D and a narrowing of the lock-in synchronization range. As the cylinder approaches the free surface, the growth of oscillation amplitude within the lock-in regime becomes more gradual compared with the abrupt amplitude increase observed for deeply submerged configurations. In unbounded flow, synchronization occurs when the vortex shedding frequency matches the natural frequency of the system, whereas in the presence of a free surface the oscillation frequency exceeds the Strouhal frequency. At near-critical Froude numbers, the transition from a vortex street to a re-circulation dominated wake leads to

suppression of vortex-induced vibrations, with A/D tending toward zero. It is hypothesized that the observed bifurcation is driven by a change in the dominant instability mechanism caused by the coupled interaction between free-surface deformation and wake dynamics, which alters the global stability characteristics of the flow. These changes in the flow global characteristics, manifested in its dynamic instability, require separate, more detailed investigation.

REFERENCES

[1] Williamson C. H. K., R. Govardhan (2004) Vortex-induced vibrations, Annu. Rev. Fluid Mech., **36**, 413–455.

[2] Sarpkaya T. (2004) A critical review of the intrinsic nature of vortex-induced vibrations, J. Fluids Struct., **19**(4), 389–447.

[3] Bernitsas M. M., K. Raghavan, Y. Ben-Simon et al. (2008) VIVACE (Vortex Induced Vibration Aquatic Clean Energy): A new concept in generation of clean and renewable energy from fluid flow, J. Offshore Mech. Arctic Eng., **130**(4), 041101.

[4] Bearman P. W., M. M. Zdravkovich (1978) Flow around a circular cylinder near a plane boundary, J. Fluid Mech., **89**, 33–47.

[5] Sheridan J., J.-C. Lin, D. Rockwell (1997) Flow past a cylinder close to a free surface, J. Fluid Mech., **330**, 1–30, https://doi.org/10.1017/S002211209600328X.

[6] Hosseinalipour S., N. Hajighafoori Boukani (2018) Numerical investigation of vortex-induced vibrations of an elastically-mounted circular cylinder beneath a free surface, Amirkabir J. Mech. Eng., **50**(4), 727–740.

[7] Latifkar P., E. Izadpanah, S. H. Meraji et al. (2024) Numerical study of vortex-induced vibrations in two cylinders near a free surface, Ocean Eng., **314**, 119762, https://doi.org/10.1016/j.oceaneng.2024.119762.

[8] Crespo A. J. C., J. M. Dominguez, B. D. Rogers et al. (2015) DualSPHysics: Open-source parallel CFD solver based on smoothed particle dynamics (SPH), Comput. Phys. Commun., **187**, 204–216.

[9] Domínguez J. M., G. Fourtakas, C. Altomare et al. (2022) DualSPHysics: from fluid dynamics to multiphysics problems, Comput. Part. Mech., **9**(5), 867–895, https://doi.org/10.1007/s40571-021-00404-2.

[10] Zhao F., H. Zhu, P. Huan et al. (2025) Vortex-induced vibration of two circular cylinders in tandem near a free surface, Phys. Fluids, **37**(9), 093605.

[11] ITTC (2021) ITTC Recommended Procedures and Guidelines: Uncertainty Analysis in CFD, International Towing Tank Conference. https://www.ittc.info/media/8187/76-01-01.pdf

[12] Rider W. J., D. B. Kothe (1998) Reconstructing volume tracking, J. Comput. Phys., **141**, 112–152.

[13] Pope S. B. (2000) Turbulent Flows, Cambridge, Cambridge University Press, 771 pp.

[14] Jeong J., F. Hussain (1995) On the identification of a vortex, J. Fluid Mech., **285**, 69–94.

[15] Blevins R. D. (1990) Flow-Induced Vibration, New York, Van Nostrand Reinhold, 324 pp.
[16] Huerre P., P. A. Monkewitz (1990) Local and global instabilities in spatially developing flows, Annu. Rev. Fluid Mech., **22**, 473–537.

Institute of Metal Science, Equipment, and Technologies with Hydro- and Aerodynamics Centre "Acad. A. Balevski", Bulgarian Academy of Sciences, 1 William Froude St, P.O. Box 58, 9000 Varna, Bulgaria
e-mails: g.nikolov@bshc.bg, trukhchev@yahoo.co.uk, rkishev@yahoo.com, a.anastasov@bshc.bg